BUILDING FIRE BEHAVIOUR IMPLEMENTING GYPSUM PLASTERBOARDS CONTAINING PHASE CHANGE MATERIALS: A CFD STUDY

Dionysios I. Kolaitis[1], Eleni K. Asimakopoulou[2] and Maria A. Founti[3]

Laboratory of Heterogeneous Mixtures and Combustion Systems, Thermal Engineering Section,
School of Mechanical Engineering, National Technical University of Athens, Greece.
[1]e-mail: dkol@central.ntua.gr, [2]e-mail: elasimak@central.ntua.gr, [3]e-mail: mfou@central.ntua.gr;
web page: http://hmcs.mech.ntua.gr

Keywords: CFD, Fire, Gypsum plasterboard, Phase Change Material.

Abstract. *The incorporation of Phase Change Materials (PCM) into building elements may affect favourably the overall building energy consumption. Common PCM added to gypsum plasterboards consist of paraffins. In the event of a fire, building elements may be exposed to substantially high temperatures; paraffins, exhibiting relatively low boiling points, may evaporate and, escaping through the plasterboard's porous structure, emerge to the fire region, where they may ignite, thus adversely affecting the fire resistance characteristics of the building. In this study, detailed numerical simulations of the developing flow and thermal fields in a model room exposed to fire conditions are performed using a CFD tool; the turbulent flow is described using the LES approach. The impact of PCM addition to the overall fire behaviour of gypsum plasterboards is investigated by means of a parametric study; the model room is assumed to be clad with either "plain" gypsum plasterboards or PCM-enriched gypsum plasterboards. Detailed predictions of the temporal evolution of wall surface temperature, gas mixture velocity and temperature, species concentrations and smoke movement are utilized to assess the effect of PCM addition to the gypsum plasterboard.*

1 INTRODUCTION

Uncontrollable fires in buildings represent a significant part of fire-related fatalities [1]. Investigation of the commonly used building materials' fire behaviour is of primary interest since the developed thermal environment and the production of toxic gases are associated with a large range of hazards to human life and properties. In building fires, the confined space controls the ventilation conditions and affects the developing thermal field, thus influencing the thermal exposure of structural elements [2, 3]. In recent years, a variety of numerical techniques have been developed in order to enable the prediction of fire growth and smoke movement within enclosures, utilizing Computational Fluid Dynamics (CFD) software as important fire engineering tools [4, 5, 6]. Recent advances in CFD techniques allow the numerical solution of the fundamental equations of mass, momentum and energy transfer in an enclosure fire environment [7]; the role of CFD tools is steadily increasing as the models become progressively robust and sophisticated. As a result, the CFD approach is considered to be fundamental to the future development of fire models, which can provide the basis for performance-based fire safety regulations.

The incorporation of Phase Change Materials (PCM) into building materials has been investigated as a way of increasing the thermal mass of building elements [8]. This innovative technique takes advantage of the latent heat of the PCM during the solid-to-liquid phase change to stabilize the temperature of the material and reduce the heat losses/gains from the building to the environment [9]. PCM can be incorporated in concrete, gypsum plasterboards, plaster and other building materials. Micro-encapsulation of the PCM prior to incorporation to the building material has been favoured in commercial applications[10-11]. In this case, PCM are contained in spherical capsules, which range in size from 1μm to 300μm; the capsules can be formulated using a wide variety of materials, including natural and synthetic polymers [12]. In commonly used PCM, the solid-liquid phase change occurs in the typical temperature range found indoors (20-26°C), which is favourable for building energy consumption purposes. However, in the unlikely event of a fire, building materials may be exposed to substantially higher temperatures, that may even reach 800°C. In this case, paraffin-based PCM are expected to evaporate, since the boiling point of typical paraffins lies below 350°C. As a result, if the PCM encapsulation shell is broken, due to the high temperature environment, the produced paraffin vapours may be released to the porous structure of the gypsum plasterboard and, through mass diffusion processes, emerge to the main combustion region. In this case, paraffin vapours are expected to ignite, thus adversely affecting the building's fire resistance characteristics [13]. The impact of this effect is investigated in the current study, using a CFD tool to simulate a model room exposed to fire conditions.

2   NUMERICAL SIMULATION METHODOLOGY

2.1   The FDS Code

The numerical simulations are performed using the Fire Dynamic Simulator (FDS, Version 5.5.3), which is a code developed by NIST [14]. The FDS code is a CFD tool capable of studying fundamental fire dynamics and combustion, aimed at solving practical fire problems in fire protection engineering. The FDS code solves numerically a form of the Navier-Stokes equations appropriate for low-speed, thermally driven flows, emphasizing on smoke production and heat transfer from fires. The approximation involves the filtering out of acoustic waves while allowing for large variations in temperature and density. This gives the equations an elliptic character. The partial derivatives of the conservation equations of mass, momentum and energy are approximated as finite differences and the solution is updated in time on a three-dimensional, Cartesian grid. Scalar quantities are assigned in the centre of each grid cell and vector quantities are assigned at the respective cell faces. The core algorithm is a semi-implicit (explicit in velocity and implicit in pressure) predictor-corrector scheme that is second order accurate in space and time by using central differences. In the first predictor step, FDS computes a rough approximation of the thermodynamic quantities that are necessary in order to be able to proceed to the next time step. At the next time step, the velocity is estimated using a new pressure term from the solution of the Poisson equation. Based on this estimation of velocity, a corrector step modifies the thermodynamic quantities and computes the corrected velocity using a recomputed pressure term. The numerical scheme in FDS requires the solution of the Poisson equation for the computation of the pressure twice within a time iteration.

Turbulence is described by using the Large Eddy Simulation (LES) approach. A filtration procedure is employed using the characteristic grid cell length as the filter width. Averaging is only performed for turbulent fluctuations exhibiting length scales smaller than the filter width and a subgrid turbulence model is used for the small-scale turbulent viscosity. The subgrid-scale turbulence is simulated using the Smagorinsky model, utilizing a Smagorinsky constant value of 0.2. Another coefficient is the sub-grid scale turbulent Prandtl number (Pr_t), which is normally determined by empirical correlations within the range of 0.2-0.9. Although dynamic procedures have been created for the modelling of these parameters, most fire simulations rely on constant values of C_s, Sc_t and Pr_t. In the particular case study both turbulent Pr_t and Sc_t values were chosen to be equal to 0.5. There are no rigorous justifications for these choices other than through direct comparison with experimental data for strong buoyant flows originating from enclosure fires occurring inside compartments. Turbulent vortices with a characteristic size larger than the filter width are calculated directly from the equations. As a result, it is possible to take into account the large-scale eddy formations in flames and investigate the dominant role of the developing buoyant forces. Thermal radiation is simulated using the finite volume methodology on the same grid as the flow solver. All solid surfaces are assigned thermal boundary conditions by taking into account information about the burning behaviour of the respective material. The time step is dynamically adjusted in order to satisfy the CFL criterion. The CFL condition asserts that the solution of the equations cannot be updated with a time step larger than that allowing a parcel of fluids to cross a grid cell. For most large-scale calculations where convective transport dominates diffusive, the CFL condition restricts the time step.

The FDS code has undergone extensive validation studies [14, 15]. The model room geometry used in this work is identical to the room used in a series of experiments, performed in the NIST Large Fire Research Laboratory [16, 17]; predictions of the FDS code have been found to exhibit good quantitative agreement with the measured temporal profiles of the gas temperature, instantaneous heat release rate and O_2, CO_2 and CO volume concentrations [16, 17, 18].

2.2   Physical Dimensions of the Model Room

In order to investigate the effect of PCM addition to the fire behaviour of gypsum plasterboards, a model room geometry is utilized; the model room is identical to the room used in the standard "Room Corner Test" (ISO 9705). The main room dimensions are 2.4 m x 3.6 m x 2.4 m; a 0.8 m x 2.0 m open door is located on a rectangular side wall (Figure 1). The fire source is assumed to be a rectangular (1.0 m x 1.0 m) burner, fed with n-heptane, located at the geometrical centre of the room (Figure 1); the considered geometry corresponds to the experimental arrangement, used in the NIST Large Fire Research Laboratory [16, 17].
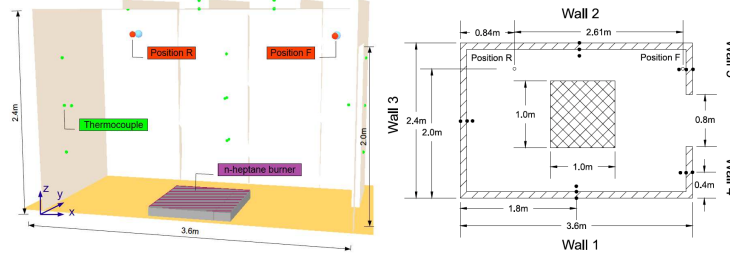
Figure 1. General configuration (left) and top section view (right) of the model room.

2.3 Computational Grid and Boundary Conditions

In the context of enclosure fire simulations, the quality of the utilized grid resolution is commonly assessed utilizing the non-dimensional $D^*/\delta x$ ratio, where D^* is a characteristic fire diameter and δx corresponds to the nominal size of the grid cell. D^* can be estimated using Equation (1), which involves a variety of physical quantities, such as the total heat release rate (Q), the ambient density (ρ), specific heat (C_p) and temperature (T).

$$D^* = \left(\frac{Q}{\rho_\infty C_{P,\infty} T_\infty \sqrt{g}} \right)^{2/5} \quad (1)$$

The $D^*/\delta x$ ratio corresponds to the number of computational cells spanning D^* and is representative of the adequacy of the grid resolution. If the value of the $D^*/\delta x$ ratio is sufficiently large, the fire can be considered well resolved. Several studies have shown that values of 10 or more are required to adequately resolve most fires and obtain reliable flame temperatures [19, 20]. In the current study, a 2000 kW fire was considered; in order to ensure that the $D^*/\delta x > 10$ criterion is fulfilled but, at the same time, to reduce the required computational cost, a nominal 0.1 m cell size was selected. In FDS, fire is represented using the "mixture-fraction" combustion model. The actual combustion process in the fire is not simulated. As a result, a basic assumption in the model is that the reaction of fuel and oxygen is infinitely fast (fuel and oxygen cannot co-exist and they will react at any temperature).

The selected numerical grid consists of 8 computational meshes (Figure 2), thus allowing the utilization of the "parallel" version of the FDS code. The numerical grid extends to the outside of the enclosure, in order to effectively simulate air entrainment phenomena. The size of the physical domain extensions, 2 m in the y- and 4.5 m in the z-direction, have been selected following suggestions found in a relevant study on the effect of computational domain size on numerical simulation of building fires [18]. Each computational mesh consists of 10 x 30 x 45 cubic (0.1 m side) cells; the total number of computational cells is 108,000.
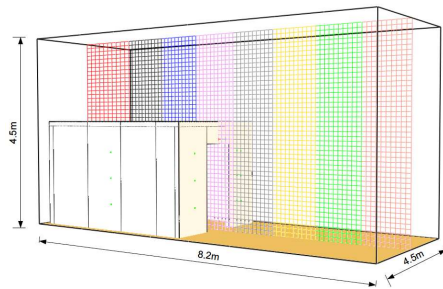

Figure 2. Physical domain and utilized computational meshes.

In the present study, the n-heptane burner is assumed to operate under steady-state conditions; the respective thermal power is equal to 2000 kW. The soot yield, which represents the fraction of n-heptane fuel mass converted to smoke particulates, is set equal to 1.5 %, according to available measurements [15]. The total simulation time is selected to be equal to 5 min, thus allowing sufficient time for the fire to reach its fully developed stage. At the beginning of the numerical simulation ($t = 0$ s), the entire computational domain (both indoors and outdoors) is assumed to be still (zero velocity), exhibiting a temperature of 20°C. Open boundaries are imposed at all boundaries external to the enclosure and wall boundary conditions are used at walls, ceiling and floor.

A parametric study, focusing on the impact of PCM addition on the fire characteristics of gypsum

plasterboards is performed, utilizing two test cases; all simulation parameters are identical, except from the material used to construct the model room walls. In the first test case (GP), 25 mm "conventional" gypsum plasterboards are used to clad the room walls, whereas in the second test case (GP+PCM), paraffin-based PCM are assumed to be incorporated to the 25 mm gypsum plasterboards. Detailed temperature-dependent physical properties of gypsum plasterboards are used to describe their thermal behaviour. The simulations are performed using a 6 GB RAM, Core i7 920 Processor, desktop PC; each simulation lasted approximately 24 hours.
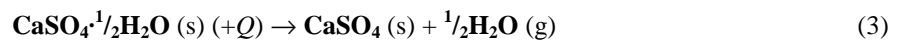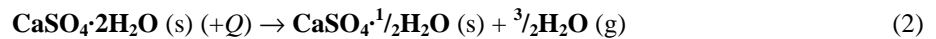
3 FIRE BEHAVIOUR OF BUILDING MATERIALS

In order to improve the prediction quality in fire simulation studies, a detailed knowledge of the thermo-physical properties and kinetic parameters, associated with the fire behaviour of the respective building materials, is required. In this context, detailed measurements using both Differential Scanning Calorimetry (DSC) and Thermo Gravimetric Analysis (TGA) have been performed in order to determine the thermo-physical behaviour of the considered building materials at elevated temperatures and intense heating rates.

3.1 Gypsum Plasterboards

Gypsum plasterboards are widely used in the building industry for a variety of applications as an aesthetically pleasing, easily applied and mechanically enduring facing material for walls and ceilings. In the context of building fire safety, gypsum plasterboards are capable of decelerating the penetration of fire through walls and floors, due to the endothermic gypsum dehydration process occurring in high temperatures. When gypsum plasterboard is subjected to a high temperature environment, water molecules bound in its crystal lattice are released and transferred through the board, absorbing energy and thus reducing the mean wall temperature. This process is known to improve the global fire resistance of the building and it is suggested to enhance the safety margins of the building, by allowing longer evacuation times [21].

A typical gypsum plasterboard contains mainly gypsum, which consists mainly of calcium sulphate dihydrate ($CaSO_4 \cdot 2H_2O$), i.e. calcium sulphate with 21% (by weight) chemically bound water. In addition, gypsum usually contains a small amount of absorbed water, as well as calcium carbonate ($CaSO_4$). When gypsum is heated above 90°C, the chemically bound water dissociates from the crystal lattice and evaporates. This process, known as gypsum "dehydration", occurs in the temperature region between 90°C and 250°C, depending on the heating rate; dehydration reactions are strongly endothermic, thus requiring large amounts of heat [22]. The dissociation of the chemical bound water takes place in two stages. In the first stage (Equation 2), the calcium sulphate dihydrate loses 75% of its water, thus forming calcium sulphate hemi-hydrate ($CaSO_4 \cdot \frac{1}{2}H2O$). If the gypsum plasterboard is further heated, a second reaction occurs (Equation 3), where the calcium sulphate hemi-hydrate loses the remaining water to form calcium sulphate anhydrate ($CaSO_4$). Both reactions are endothermic and absorb large amounts of energy.

$$CaSO_4 \cdot 2H_2O \text{ (s) } (+Q) \rightarrow CaSO_4 \cdot {}^1\!/_2 H_2O \text{ (s) } + {}^3\!/_2 H_2O \text{ (g)} \tag{2}$$

$$CaSO_4 \cdot {}^1\!/_2 H_2O \text{ (s) } (+Q) \rightarrow CaSO_4 \text{ (s) } + {}^1\!/_2 H_2O \text{ (g)} \tag{3}$$

The physical properties of gypsum vary with increasing temperature, due to the occurring dehydration reactions. The utilization of temperature-dependent physical properties is known to yield more accurate results in heat transfer simulations of gypsum plasterboards, compared to mean values [23] and therefore, temperature-dependent values for the thermal conductivity and specific heat were used in the simulations. The respective values have been obtained by using a 'CT-METRE' measuring device [24] and DSC analysis (Figure 3).
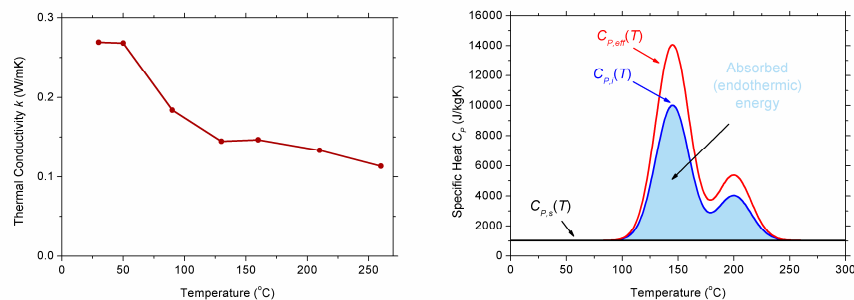

Figure 3. Temperature dependent thermo-physical properties of gypsum plasterboard.

Both gypsum dehydration and water vapour diffusion have a strong impact on the heat transfer characteristics of gypsum plasterboards exposed to fire conditions. In order to implement these effects in the utilized CFD code, a detailed solution of the respective heat and mass transfer equations across the width of the gypsum plasterboard would be required; since the computational cost of such simulations is currently prohibitive, an alternative methodology is followed. The effects of the aforementioned transport phenomena are incorporated into the specific heat values, thus constructing an "effective" specific heat temperature profile, which is then utilized in the simulations. The effective specific heat of the gypsum plasterboards is determined using Equation (4). $C_{P,s}$ stands for the "original" specific heat value of gypsum plasterboard, whereas the $C_{P,i}$ values correspond to the additional "effective" specific heats owed to the dehydration endothermic reactions occurring in elevated temperatures; the integral of each additional specific heat is equal to the energy absorbed in the respective reaction. The $C_{P,i}$ values have been estimated using DSC measurements of actual gypsum plasterboards. The f_i parameters correspond to mass transfer correction factors, which take into account the effects of vapour migration in the gypsum porous structure. The, in-house developed, HETRAN simulation tool [22], which models the simultaneous heat and mass transfer inside porous materials, has been used to define the values of the mass transfer correction factors; their values were found to be approximately 1.45, corresponding to a 45% increase of the total dehydration energy. The temperature dependent "effective" specific heat values used in the simulations are depicted in Figure 3.

$$C_{P,eff}(T) = C_{P,s}(T) + \sum_{i=1}^{N} f_i C_{P,i}(T) \tag{4}$$

3.2 Paraffin-Based Phase Change Materials

The thermal behaviour of commercial gypsum plasterboards with encapsulated paraffin-based PCM has been investigated by performing DSC measurements using an inert purge gas (nitrogen) at intense heating rates (40 K/min and 80 K/min), in order to accurately simulate fire conditions. However, further DSC measurements using a modest heating rate of 0.5 K/min were also performed, aiming to identify the different chemical reactions occurring in the PCM-enriched gypsum plasterboard sample. Commercially available paraffin-based PCM contain a large variety of paraffinic species, thus allowing better control of the overall thermal behaviour. In the examined sample, the melting energy of the PCM was found to correlate favourably to that of octadecane ($C_{18}H_{38}$, exhibiting a 27.85^{o}C melting point). As a result, the octadecane liquid-to-vapour phase change (Equation 5) is implemented in the CFD code, in order to effectively simulate the fire behaviour of the PCM-enriched gypsum plasterboard. In the simulations, "worst-case scenario" conditions have been assumed; all the encapsulating shells were considered to fail, thus allowing the entire quantity of PCM to be released in the fire region.

$$\mathbf{C_{18}H_{38}} \text{ (l)} \rightarrow \mathbf{C_{18}H_{38}} \text{ (g)} \tag{5}$$

3.3 Simulation Parameters of Solid-Phase Reactions

In the FDS code, the various solid-phase reactions (e.g. pyrolysis, dehydration etc.) are simulated using an Arrhenius equation formulation. The respective Arrhenius parameter values, used in the simulations, as well as the various species yields, are shown in Table 1. TGA thermo-analytical measurements were used to estimate the kinetic parameters, assuming unity reaction order. In the PCM-enriched gypsum plasterboard, the evaporation of paraffin is incorporated as an additional reaction of the gypsum plasterboard mass, occurring at 295°C. According to the performed DSC analysis, 18% of the initial gypsum plasterboard's mass can be transformed to PCM vapours, which eventually contribute to the enhancement of the fire load.

Reaction	Eq. (2)	Eq. (3)	Eq. (5)
Pre-exponential factor A (s^{-1})	1.353779	0.456201	0.00839
Activation energy E (kJ/kmol)	2.46x10^4	2.28x10^4	6.532x10^4
(Endothermic) Heat of reaction (kJ/kg)	345	115	207.11
Water yield (kg H_2O / kg mixture)	12.75%	4.87%	-
Residue yield (kg residue / kg mixture)	87.25%	95.13%	82%
Fuel yield (kg fuel / kg mixture)	-	-	18%

Table 1: Utilized kinetic parameters for the two-step dehydration process of gypsum and PCM release.

4 RESULTS AND DISCUSSION

4.1 Predictions of the Developing Flow-Field

Two characteristics time snapshots of the developing flow field and the respective predicted flame shape and location, 8 s and 300 s after fire initiation, are depicted in Figure 4. Both examined cases exhibit similar characteristics during the initial phase; however, paraffin vapour evaporation in case GP+PCM results in a significant enhancement of the fire intensity at the end of the simulation (300 s), compared to the GP case. The main structure of the developing flow-field is similar in both cases. As expected, a typical thermal buoyant flow is established, thus generating a strong upward flow of the heated combustion products. The required oxygen to sustain the combustion reactions is provided by air entrainment through the lower part of the opening. The flame shape and location in case GP is similar to a typical pool fire burning in the open environment; however, the growing recirculation zone, due to the air entrainment near the opening, leads to a slight deformation of the flame shape, which results in a "drift" towards the "rear" side of the enclosure. In the GP+PCM case, the additional fuel provided by the paraffin vapour release increases the thermal power, thus resulting in a larger flame and a stronger buoyant plume flow. Compared to the GP case, the observed recirculation region is more intense; the flame shape is significantly deformed, reaching the rear enclosure wall.
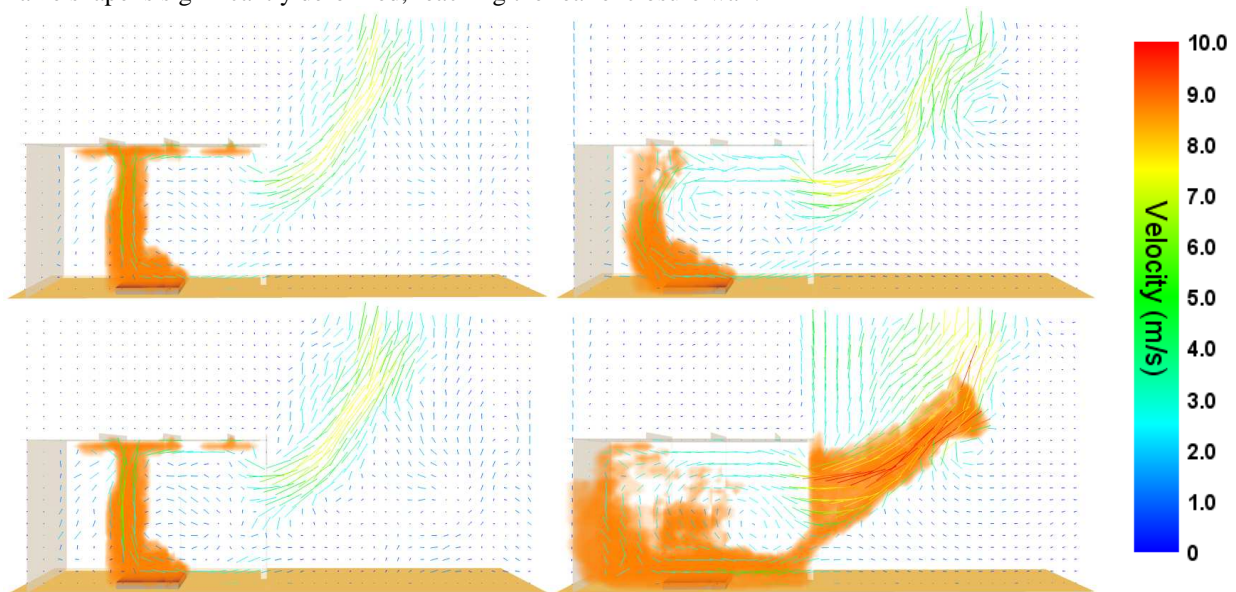

Figure 4. Predictions of gas mixture velocity and flame location, for test cases GP (top) and GP+PCM (bottom), 8 s (left) and 300 s (right) after fire initiation.

In order to investigate the characteristics of paraffin vapour evaporation, an additional simulation of case GP+PCM was performed, this time considering the produced PCM vapours as "inert media". The gradual heating of the walls results in temperatures higher than 295°C; in this case, the paraffin-based PCM, encapsulated in the gypsum plasterboard, is considered to evaporate and diffuse to the main flow region. Predictions of the temporal evolution of $C_{18}H_{38}$ vapour volume fractions are shown in Figure 5; it is evident that a significant amount of "combustible" paraffin vapours is produced, thus resulting in the enhancement of fire intensity, observed in Figure 4.
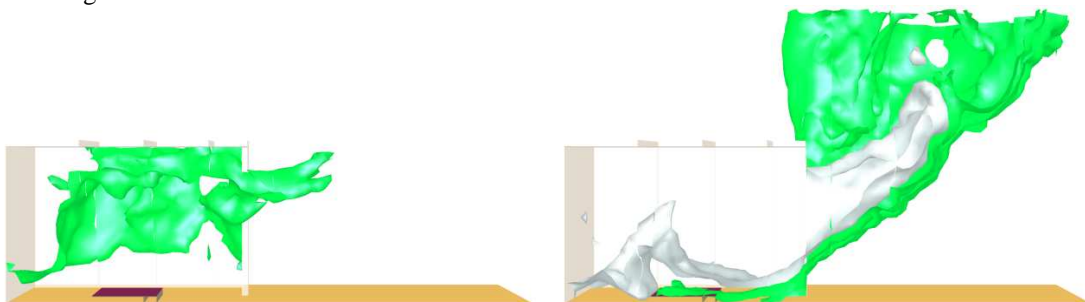

Figure 5. Predictions of $C_{18}H_{38}$ vapour volume fraction iso-surfaces (white: 0.001, green: 0.01), 35 s (left) and 300 s (right) after fire initiation.

4.2   Predictions of the Developing Thermal-Field

Predictions of the gas mixture temperature at the end of the simulation period are depicted in Figure 6, for both the examined test cases. The effect of paraffin vapour release is evident, since the observed gas temperatures in the GP+PCM case are significantly higher than the respective values of the GP case. In fact, the hot gas layer formed in the upper part of the compartment exhibits a considerable increase in height when the PCM-enhanced gypsum plasterboards are utilized.
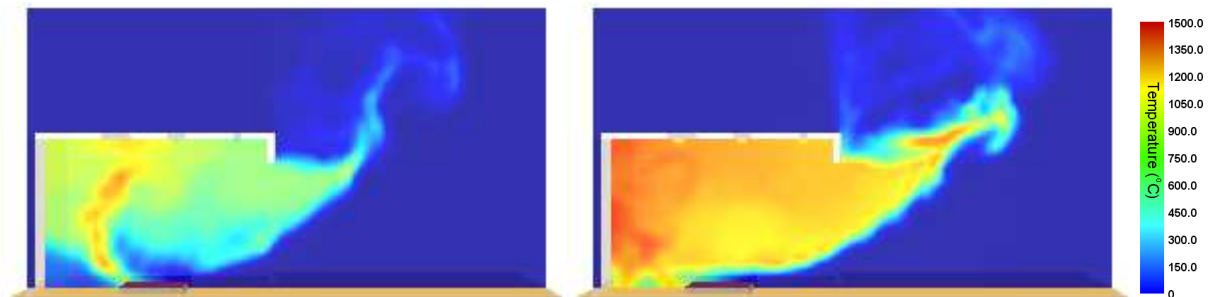

Figure 6. Predictions of gas mixture temperature 300 s after fire initiation, for test cases GP (left) and GP+PCM (right).

CFD tools allow the estimation of the fire resistance characteristics of the entire compartment and the constitutive building elements. In this context, the performed simulations are used to investigate the mechanical strength of the utilized gypsum plasterboard wall assemblies. Gypsum plasterboards exposed to fire are considered to exhibit mechanical failure when cracks or openings are observed through the wall [25]; however, since cracking phenomena cannot be accurately simulated in the FDS code, alternative failure criteria have been used in this study. According to the Australian Standard AS1530.4 [26], a gypsum plasterboard wall is considered to "fail" when the maximum temperature rise (compared to the ambient temperature) of its ambient facing side (unexposed side) exceeds 180°C. In the current simulations, the ambient temperature was considered to be 20°C; therefore, the aforementioned "failure" criterion for a gypsum plasterboard assembly corresponds to a temperature of 200°C on its unexposed side. Predictions of wall surface temperature, across a section of the exposed side of Wall 2 and the unexposed side of Walls 4 and 5 (c.f. Figure 1), for both test cases are shown in Figure 7. Temperature predictions of the wall surface directly exposed to fire are noticeably higher than the corresponding of the unexposed side. As expected, the observed wall temperatures are generally higher in the case of PCM-enriched gypsum plasterboards.
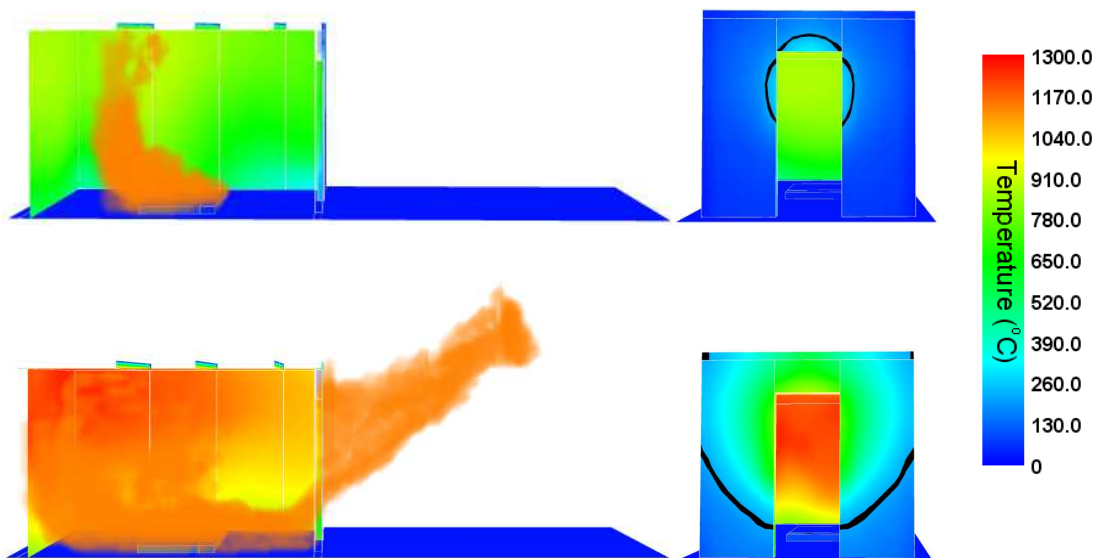

Figure 7. Predictions of exposed (left) and unexposed (right) wall surface temperatures and flame location 300 s after fire initiation, for test cases GP (top) and GP+PCM (bottom).

In both cases, the temperature of the unexposed sides of Walls 4 and 5, surrounding the opening, exceed the critical "failure" limit of 200°C; however, while in the GP+PCM case the temperature limit is reached 60 s after fire initiation, in the GP case mechanical failure of the wall is observed after 240 s of simulation time (Figure 8).
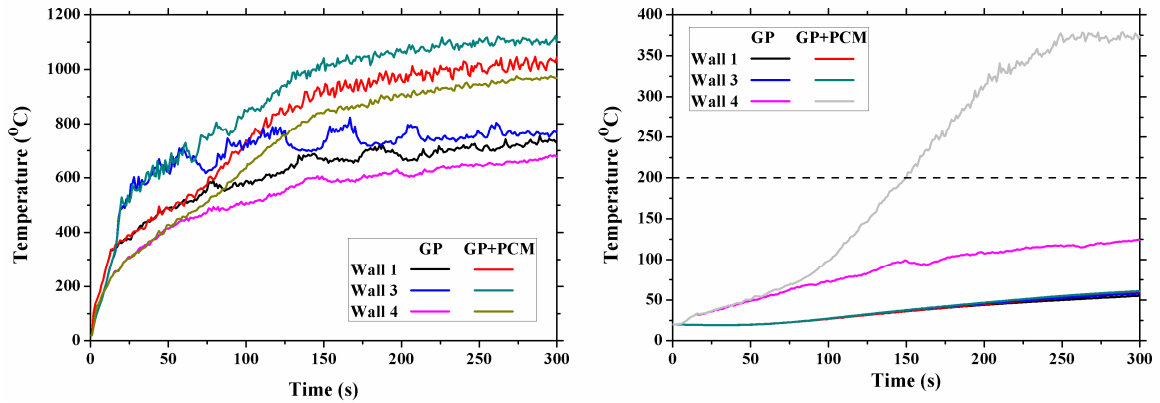

Figure 8. Temporal evolution of exposed (left) and unexposed (right) surface temperature for Walls 1, 3 and 4 at a height of 1.2 m.

4.3   Tenability Limits

In order to evaluate life safety in fire conditions using a numerical modelling tool, quantitative tenability criteria are needed. Tenability limits for incapacitation or death due to exposure to common gaseous products of combustion are presented in Table 2 [27].
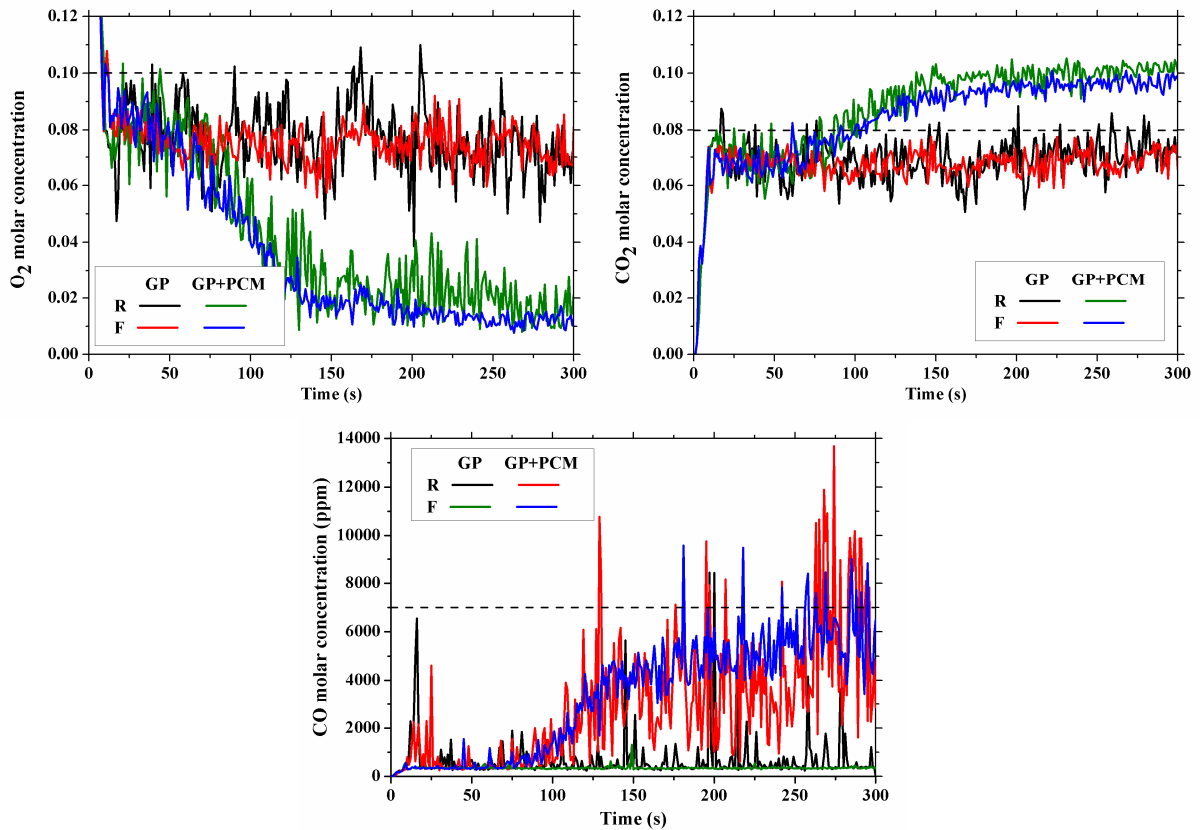

Figure 10. Temporal evolution of O_2 (top left), CO_2 (top right) and CO (bottom) molar concentrations at a height of 2.0 m.

Predictions of CO, O_2 and CO_2 volume concentration in the front (FL) and rear (RL) location of the

compartment are presented in Figure 10. In general, CO and CO_2 molar concentrations in the GP+PCM case are higher than the GP case and the respective O_2 predictions are lower, thus corroborating the enhanced fire intensity observed when PCM-enhanced gypsum plasterboards are used. The fluctuations observed in the local concentrations of the gaseous species are associated with the dynamic nature of the flow, which is owed both to flame "puffing" and the periodic entrainment of fresh air. O_2 concentration incapacitation limits are exceeded in both cases, just a few seconds in the simulation; however, "death" limits are exceeded only in case GP+PCM. Incapacitation limits regarding the CO_2 concentrations are exceeded only for case GP+PCM; CO concentrations remain, in general, lower than the corresponding "critical" values.

Gaseous species	Incapacitation	Death
CO	6,000-8,000 ppm	12,000-16,000 ppm
O_2	10-13%	< 5%
CO_2	7-8%	> 10%

Table 2: Reported volume concentration tenability limits for 5 min exposure to common combustion products.

5   CONCLUSIONS

Phase change materials have been considered as a thermal mass component in building elements for more than a decade. Today, commercial products are available where PCM are incorporated in e.g. gypsum plasterboards, aiming to enhance the energy behaviour of the building. Paraffin-based PCM generally perform well, but may compromise the fire resistance of the building. Macro- and micro-encapsulation of the PCM partly solves this problem but the major barrier for this technology is increased flammability of the utilized paraffins.

The impact of PCM addition to the fire behaviour of gypsum plasterboard systems has been investigated by using a CFD tool to simulate the flow- and thermal-fields developing in an ISO 9705 compartment during a fire. The walls of the compartment were assumed to be constructed using two alternative drywall system configurations, one exhibiting common gypsum plasterboards and the other using gypsum plasterboards enriched with PCM. Predictions of gas velocities, gas and wall temperatures and gaseous species concentrations revealed that, under the worst case scenario considered in this work, when exposed to fire conditions, paraffin vapours may be released to the main combustion area, enhancing the fire intensity; as a result, both building element fire resistance and occupant tenability may be compromised. Hence, in order for this innovative technology to have a wide spread commercial penetration in the building material market, either non-flammable PCM should be used, or new fire-resistant materials for the micro-encapsulation shells should be developed.

6   ACKNOWLEDGEMENTS

REFERENCES

[1] Yeoh, G.H., Yuen, K.K. (2009), *Computational Fluid Dynamics in Fire Engineering*, Elsevier.

[2] Quintiere, J.G. (2002), "Fire behavior in building compartments", *Proceedings of the Combustion Institute*, Vol. 29, pp. 181-193.

[3] Merci, B., Van Maele, K. (2008), "Numerical simulation of full-scale enclosure fires in a small compartment with natural roof ventilation", *Fire Safety Journal*, Vol. 43, pp. 495-511.

[4] Olenick, S.M., Carpenter, D. (2003), "An updated international survey of computer models for fire and smoke", *Journal of Fire Protection Engineering*, Vol. 13, pp. 611-666.

[5] Makhviladze, G.M., Shamshin, A.V., Yakush, S.E. and Zykov, A.P. (2006), "Experimental and numerical study of transient compartment fires", *Combustion, Explosion and Shock Waves*, Vol. 42, pp. 723-730.

[6] Wen, J.X., Kang, K., Donchev, T. and Karwatzki, J.M. (2007), "Validation of FDS for the prediction of medium scale pool fires", *Fire Safety Journal*, Vol. 42, pp. 127-138.

[7] Novozhilov, V. (2001), "Computational fluid dynamics modeling of compartment fires", *Progress in Energy and Combustion Science*, Vol. 27, pp. 611-666.

[8] Agyenim, F., Hewitt, N., Eames, P. and Smyth, M. (2010), "A review of materials, heat transfer and phase change problem formulation for latent heat thermal energy storage systems (LHTESS)", *Renewable and Sustainable Energy Reviews*, Vol. 14, pp. 615-628.

[9] Voelker, C., Kornadt, O. and Ostry, M. (2008), "Temperature reduction due to the application of phase change materials ", *Energy and Buildings*, Vol. 40, pp. 937-944.

[10] Mandilaras, I., Founti, M.A. (2009), "Experimental investigation of agglomerate marbles containing phase change materials", *Proceedings of the 11th International Conference on Thermal Energy Storage (Effstock)*, Stockholm, Sweden, 14-17 June 2009.

[11] Hunger, M., Entrop, A.G., Mandilaras, I., Brouwers, H.J.H. and Founti, M. (2009), "The behavior of self-compacting concrete containing micro-encapsuled Phase Change Materials", *Cement and Concrete Composites*, Vol. 3, pp. 731-743.

[12] Hawlader, M.N.A., Uddin, M.S., Khin, M.M. (2003), "Microencapsulated PCM thermal-energy storage system", *Applied Energy*, Vol. 74, pp. 195-202.

[13] Kosny, J., Yarbrough, D.W., Riazzi, T., Leuthold, D., Smith, J.B. and Bianchi, M. (2009), "Development and testing of ignition resistant microencapsulated phase change material", *Proceedings of the 11th International Congress on Thermal Energy Storage (Effstock)*, Stockholm, Sweden, 14-17 June 2009.

[14] McGrattan, K., Hostikka, S. and Floyd, J. (2010), *Fire Dynamics Simulator User's Guide*.

[15] McGrattan, K. (2007), "Verification and validation of selected fire models for nuclear power plant applications, volume 7: Fire Dynamics Simulator (FDS)", *Final Report*, NUREG-1824, EPRI 1011999.

[16] Lock, A., Bundy, M., Johnsson, E.L., Hamins, A., Ko, G.H., Hwang, C., Fuss, P. and Harris, R. (2008), "Experimental study of the effects of fuel type, fuel distribution and vent size on full-scale underventilated compartment fires in an ISO 9705 room", *NIDT Technical Note 1603*, National Institute of Standards and Technology, Gaithersburg, MD.

[17] Hwang, C.H., Lock, A., Bundy, M., Johnsson, E. and Ko, G.H. (2010), "Studies on Fire characteristics in over- and underventilated full-scale compartments", *Journal of Fire Sciences*, Vol. 28, pp.459-486.

[18] Zhang, X., Yang, M., Wang, J. and He, Y. (2010), "Effects of computational domain on numerical simulation of building fires", *Journal of Fire Protection Engineering*, Vol. 20, pp. 225-250.

[19] Lin, C.H., Ferng, Y.M. and Hsu, W.S. (2009), "Investigating the effect of computational grid sizes on the predicted characteristics of thermal radiation for a fire", *Applied Thermal Engineering*, Vol. 29, pp. 2243-2250.

[20] McGrattan, K.B., Floyd, J., Forney, G., Baum, H. and Hostikka, S. (2002), "In improved radiation and combustion routines for a large eddy simulation fire model", *Proceedings of the 7th International Symposium of Fire Safety Science*, Worcester, MA, 16-21 June 2002, pp. 827-838.

[21] Wang, C.Y., Ang, C.N. (2004), "Effect of moisture transfer on specific heat of gypsum plasterboard at high tempratures", *Construction and Building Material*, Vol. 16, pp. 505-515.

[22] Kontogeorgos, D.A., Founti, M.A. (2010), "Numerical investigation of simultaneous heat and mass transfer mechanisms occurring in a gypsumboard exposed to fire", *Applied Thermal Engineering*, Vol. 30, pp. 1461-1469.

[23] Kontogeorgos, D.A., Kolaitis, D.I. and Founti, M.A. (2008), "Numerical modelling of heat transfer in gypsum plasterboards exposed to fire", *Proceedings of the 6th International Conference on Heat Transfer, Fluid Mechanics and Thermodynamics*, Pretoria, South Africa, 11-13 July 2008.

[24] Kontogeorgos, K., Mandilaras, I. and Founti, M. (2011), "Scrutinizing gypsum board thermal performance at dehydration temperatures", *Journal of Fire Sciences*, Vol. 29, pp. 111-130.

[25] Manzello, L.S., Gann, G.R., Kukuck, R.S. and Lenhert, B.D. (2007), "Influence of gypsum board type on real fire performance of partition assemblies", *Fire and Materials*, Vol. 31, pp. 425-442.

[26] Clancy, P. (2002), "A parametric study on the time-to-failure of Wood framed walls in fire", *Fire Technology*, Vol. 38, pp. 243-269.

[27] DiNenno, P.J., Drysdale, D., Beyler, C.L., Walton W.D., Cruster, R.L.P., Hall, J.R. and Watts, J.M. (2002), *S.F.P.E. Handbook for Fire Engineering*, 3rd Edition, National Fire Protection Association, Quincy, Massachusetts, U.S.A.